AGU PUBLICATIONS

Geophysical Research Letters

RESEARCH LETTER
10.1002/2016GL072026

Key Points:
- Frequent clusters have increased seismicity rates near the southernmost San Andreas Fault (SAF) since the 1979 Imperial Valley earthquake
- The 2001, 2009, and 2016 clusters included *M*4 events in the vicinity of the SAF but caused mostly negative Coulomb stress changes on SAF
- Triggering a major rupture on SAF that has not ruptured for ~320 years may require larger or more numerous close events

Correspondence to:
E. Hauksson,
Hauksson@caltech.edu

Citation:
Hauksson, E., M.-A. Meier, Z. E. Ross, and L. M. Jones (2017), Evolution of seismicity near the southernmost terminus of the San Andreas Fault: Implications of recent earthquake clusters for earthquake risk in southern California, *Geophys. Res. Lett.*, *44*, 1293–1301, doi:10.1002/2016GL072026.

Received 27 NOV 2016
Accepted 20 JAN 2017
Accepted article online 24 JAN 2017
Published online 9 FEB 2017

Evolution of seismicity near the southernmost terminus of the San Andreas Fault: Implications of recent earthquake clusters for earthquake risk in southern California

Egill Hauksson[1], Men-Andrin Meier[1], Zachary E. Ross[1], and Lucile M. Jones[1]

[1]Division of Geological and Planetary Sciences, Seismological Laboratory, California Institute of Technology, Pasadena, California, USA

Abstract Three earthquake clusters that occurred in the direct vicinity of the southern terminus of the San Andreas Fault (SAF) in 2001, 2009, and 2016 raised significant concern regarding possible triggering of a major earthquake on the southern SAF, which has not ruptured in more than 320 years. These clusters of small and moderate earthquakes with $M \leq 4.8$ added to an increase in seismicity rate in the northern Brawley seismic zone that began after the 1979 M_w 6.5 Imperial Valley earthquake, in contrast to the quiet from 1932 to 1979. The clusters so far triggered neither small nor large events on the SAF. The mostly negative Coulomb stress changes they imparted on the SAF may have reduced the likelihood that the events would initiate rupture on the SAF, although large magnitude earthquake triggering is poorly understood. The relatively rapid spatial and temporal migration rates within the clusters imply aseismic creep as a possible driver rather than fluid migration.

1. Introduction

Is there a reason to be concerned about possible triggering of an $M > 7$ earthquake on the SAF, when earthquake clusters occur near its southernmost terminus in the Brawley seismic zone (BSZ)? This question has been asked three times in the last 15 years. Frequent swarms, high heat flow, and crustal extension characterize the BSZ, but the southernmost SAF is mostly aseismic except where it abuts the BSZ. We attempt to provide some answers to this question derived from the available seismicity and tectonic data (Figure 1).

Numerous previous studies have shown that either small or large earthquakes can trigger other earthquakes both through static and dynamic triggering [*Hill et al.,* 1993; *Kilb et al.,* 2000; *Felzer and Brodsky,* 2006]. In particular, because small earthquakes are so numerous their influence on the redistribution of elastic stresses and the triggering of following earthquakes can be significant [*Hanks,* 1992; *Helmstetter,* 2003; *Marsan,* 2005; *Meier et al.,* 2014]. Foreshocks, which precede about half of $M \geq 5.0$ main shocks in southern California [*Jones,* 1984], are often interpreted as evidence for such earthquake-to-earthquake triggering. In particular, the 1987 M_w 6.2 Elmore Ranch earthquake, located ~30 km to the southwest of Bombay Beach, is believed to have triggered the 1987 M_w 6.6 Superstition Hills earthquake within ~13 h [*Hudnut et al.,* 1989; *Bent et al.* 1989]. The two strike-slip earthquakes occurred on faults that are nearly perpendicular to one another. The BSZ swarms have a similar relative orientation to the SAF of ~90°. This type of scenario is therefore often thought of as a possible model for foreshocks in the BSZ triggering a main shock on the southern SAF. Because foreshocks by definition are preferentially located near the epicenters of their main shocks, small earthquakes located near major faults have raised extra concern for the potential to trigger large earthquakes on those faults [e.g., *Agnew and Jones,* 1991; *Michael,* 2012].

Since the early days of detailed seismic monitoring in the 1930s, frequent earthquake clusters or swarms have been recorded in the southern BSZ in Imperial Valley. The BSZ consists of a mixture of left lateral step over faults that connect short right-lateral strike-slip fault segments [*Johnson and Hill,* 1982] and is thought to accommodate the relative motion of the Pacific-North America plate boundary between the SA and Imperial faults. These swarms were all located in the southern BSZ, to the south of the Salton Sea. These onshore swarms are attributed to a small extensional component in the state of stress, possible presence of geothermal or magmatic fluids as well as lack of any major through going fault [*Hauksson et al.,* 2013; *Yang and Hauksson,* 2013].

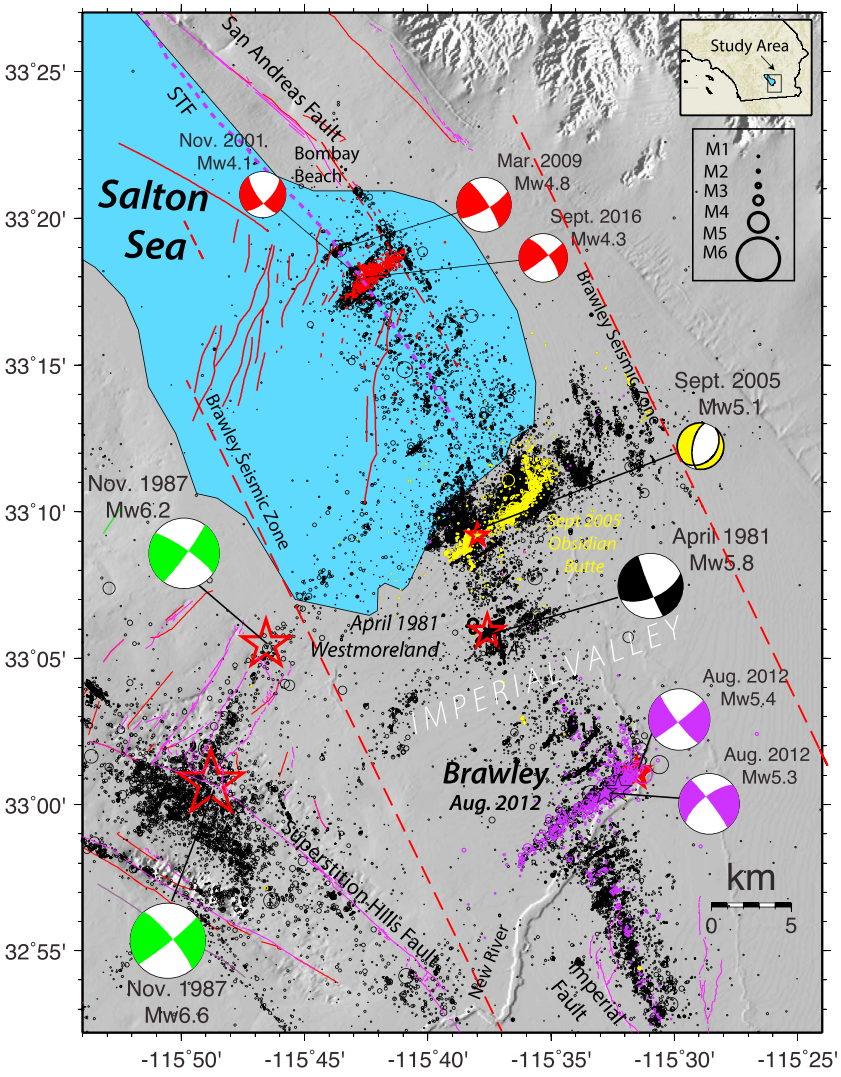

Figure 1. Map of 1981–2016 relocated seismicity of the BSZ shown as black circles. The lower hemisphere focal mechanisms for larger events that are labeled include 1981 Westmoreland, 1987 Elmore Ranch and Superstition Hills (green), Obsidian Butte 2005 (yellow), Brawley 2012 (purple), and the Bombay Beach 2001, 2009, and 2016 (red). Elmore Ranch and Superstition Hills moment tensors are from *Bent et al.* [1989] and *Yang et al.* [2012]. The late Quaternary faults are from *Jennings and Bryant* [2010]; normal faults beneath the Salton Sea and the offshore extension of the SAF are from *Brothers et al.* [2009]. The Salton Trough fault (STF) is from *Sahakian et al.* [2016].

The last major earthquake to rupture the southern SAF occurred more than 320 years ago [*Rockwell et al.,* 2016]. In comparison with the high heat flow and transtensional BSZ to the south, the Coachella segment SAF has very low rate of background seismicity, indicating that this part of the fault is locked [*Hauksson et al.,* 2012]. Furthermore, *Yang and Hauksson* [2013] showed that this section of the SAF is not favorably oriented in the local stress field, based on inversions of focal mechanisms. Nonetheless, because of the possible large risk and impact of a major SAF earthquake, any hint of renewed seismicity raises concerns. To better understand the implication of these swarms, we examine both the seismicity rate change in the northern BSZ and the static stress changes caused by the $M \geq 4.0$ events on the SAF.

2. Materials and Methods

We use the *P* and *S* phase picks determined by the Caltech/U.S. Geological Survey (USGS) Southern California Seismic Network (SCSN) to relocate all of the events in the three clusters. We applied SIMULPS to relocate the events using a 3-D velocity model modified from *Hauksson* [2000] and determine absolute errors for the hypocenters of ~0.5 km, which depend on availability of *P* and *S* picks [*Thurber,* 1993]. In the final step, we

included cross-correlation differential travel times and applied HypoDD [*Waldhauser and Ellsworth,* 2000]. Because all three clusters were relocated jointly, their relative depths are reliable.

We analyzed first motion polarities and S/P amplitudes and applied the HASH method of *Hardebeck and Shearer* [2003] to determine focal mechanisms. The clusters exhibited mostly strike-slip faulting on northwest or southwest striking nodal planes. For the $M > 4$ earthquakes, we used the human reviewed (SCSN) moment tensors [*Clinton et al.,* 2006]. The centroid depths are in the 5 km range with a resolution of ±4 km.

3. Results

3.1. Earthquake Clusters

The BSZ is the ~60 km long transtensional step over between the SAF in the north and the Imperial fault (IF) in the south [*Johnson and Hill,* 1982]. Recently *Brothers et al.* [2009] mapped a zone of hinge faults with oblique slip close to the trace of the SAF (Figure 1) using active seismic reflection techniques. These faults lie within the northernmost extent of the BSZ transitioning to the SAF, and consist of numerous short, en echelon fault segments, and mostly exhibit normal motion with the down drop block to the southeast.

Three times in the last 15 years in 2001, 2009, and 2016, clusters of small earthquakes occurred within a few kilometers distance of the southern terminus of the SAF, near the eastern part of the hinge zone faults (Figure 2). These clusters with largest magnitudes of $4.0 \leq M \leq 4.8$ were located in the depth range from 3 to 10 km about 1 to 5 km southwest of the inferred trace of the SAF but within the northern BSZ. All three clusters had strike and dip different from the hinge faults, confirming the presence of unmapped strike-slip faults. The three clusters are spatially offset from each other and appear to be on different structures (Figure 2).

The temporal and spatial evolution of the three clusters differs significantly (Figure 2c). The 2001 cluster lasted only for 24 h and formed an almost linear distribution extending from southwest to northeast. The 2009 cluster consisted of two subclusters lasting for 30 days, each with a northeast trend, but spaced ~5 km apart. The 3 day long 2016 cluster was located in between the 2001 and 2009 clusters extending for ~6 km. The rapid spatial expansion of each cluster with migration rates of up to ~2 km/h could have been caused by aseismic slip over a larger fault area, but no geodetic data are available to confirm this inference (Figure 2c).

A steady rate of background seismicity is not observed near the onshore SAF but does mark the offshore trace of the SAF since at least 1981, or the start of the high precision catalog (Figure 1). These ~390 events have magnitudes ranging from ~1.0 to 3.5 and are located within 1.5 km distance using a 3-D velocity model, mostly to the east of the inferred trace of the SAF, and thus the SAF may dip steeply to the east-northeast. This steady rate of seismicity suggests that the abutting BSZ is affecting the long-term state of stress along the offshore terminus of the SAF. However, the SAF remained locked during the three clusters because none of the three clusters seem to cause detectable aftershocks near the SAF.

3.2. Coulomb Stress Changes

To quantify potential stress changes on the southern SAF, we modeled the cumulative change in Coulomb stress that the events of the clusters imparted (Figure 3). Coulomb stress changes quantify to what extent, both shear and normal stress changes bring a medium closer to or further from failure [e.g., *Harris et al.,* 1995]. The stress changes depend on the relative orientation of source and receiver faults, directions of slip, and frictional coefficient but not on the regional stress field. We assume a coefficient of friction of 0.4, a Skempton's ratio of 0.5 and a rigidity of 20 GPa. For each earthquake we generate a square-shaped uniform slip model, assuming 3 MPa stress drop, following the procedure of *Meier et al.* [2014]. Using the computer code of *Wang et al.* [2006], we resolve the Coulomb static stress changes onto the receiver fault orientation corresponding to that of the southern SAF (strike = 325°; dip = 90°; and rake = 180°). We infer vertical dip for the SAF because the strike aligned seismicity is within 0 to 2 km distance at focal depths of ~8 to 9 km. *Fuis et al.,* [2012] inferred 59° dip of the SAF ~15 km to the north by extrapolating the SAF surface trace to seismicity located ~6 km away from the surface trace at focal depths of 8 to 10 km. Because *Fuis et al.,* [2012] showed that the dip of the SAF can vary significantly over short distances, a much steeper dip in the vicinity of Bombay Beach is permissible when compared with their interpreted dip to the north.

The resulting cumulative Coulomb stress changes caused by the events of the three clusters exhibit complicated three-dimensional distributions but are dominated by the largest events of each cluster (Figure 3). The

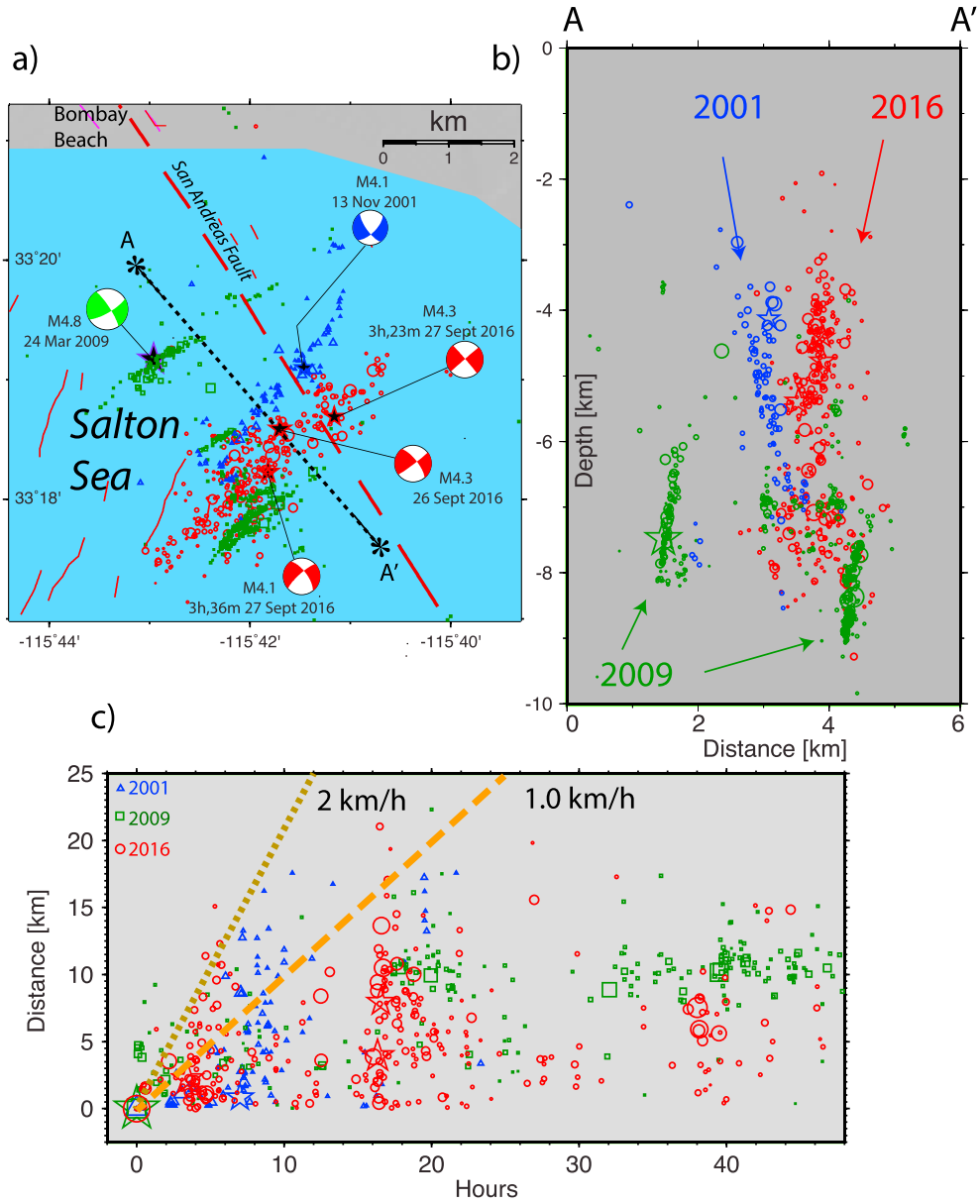

Figure 2. (a) Map view of the 2001 (blue triangles), 2009 (green squares), and 2016 (red circles) earthquake clusters, including focal mechanisms. (b) Depth section is taken along the line A-A′. (c) Distance and time from the location and origin time of the first event of each cluster. Two dashed lines indicate possible aseismic creep rate of ~1 km/h and ~2 km/h.

modeled stress changes impart both positive and negative stresses on the nearby SAF segments. In the range of possible SAF dips from 60° to 90° the Coulomb stress field does not vary significantly. Since the Salton trough fault is inferred to run roughly parallel to the SAF [*Sahakian et al.*, 2016] the modeled stress changes shown in Figure 4 are also valid for the STF.

The 2001 cluster caused the most direct stress change on the trace of the SAF over a ~2 km spatial extent because the hypocenter of the *M*4 event was located very close to the trace of the SAF. One of the main lobes of positive Coulomb stress extended to the northwest centered on the trace of the SAF. However, because of the shallow focal depth of 6 km, and because of the small size of the stress source, the stress changes at depths below 7 km are much smaller, where a $M > 7$ triggered event may be more likely to originate [*Scholz*, 2002].

The 2009 cluster was overall deeper with a main shock focal depth of the largest event (*M*4.8) at ~9 km depth. Substantial Coulomb stress changes of >0.1 MPa are modeled out to a distance of ~8 km, and they are

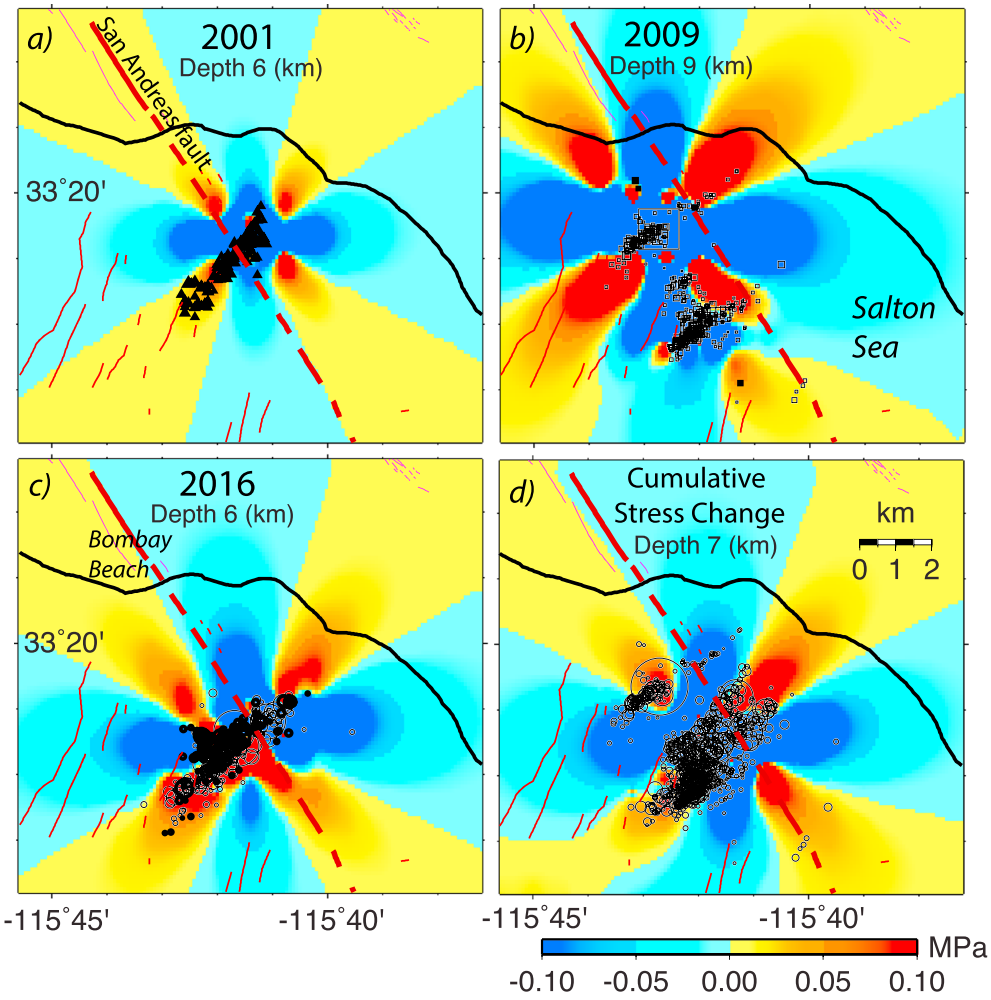

Figure 3. Cumulative Coulomb static stress changes caused by the events from each cluster at the depth of the largest event of each cluster, exerted on receiver mechanisms equivalent to the orientation of the SAF by the (a) 2001, (b) 2009, and (c) 2016 cluster. (d) The cumulative Coulomb stress change of all three clusters at 7 km depth, and the 2001, 2009, and 2016 epicenters are shown as circles.

dominated by the *M*4.8 event. High-amplitude positive stress changes on the SAF are modeled along a ~2 km long section of the fault, which are bracketed by ~3 km long negative Coulomb stress changes on both sides. The northwest main lobe of increased stress misses the SAF because the epicenter was offset by 4 km to the west away from the SAF.

The three $M > 4$ events in the 2016 cluster occurred at focal depth of ~6 km. They caused Coulomb stress changes of >0.1 MPa over ~5 km of the SAF (Figure 3). At depths above 7 km the stress changes are predominantly negative, while they are mostly positive in the depth range from 7 to 9 km. As in 2009, the main positive stress lobe extending to the northwest is offset from the SAF, suggesting that the stress changes imparted on the onshore SAF are minor.

The modeled stress changes from each of these clusters are rather small, and they are strongly dependent on uncertainties in the relative source receiver geometries [*Meier et al.,* 2014]. When summed up the three clusters substantially reduced or increased the Coulomb stress on the SAF only over a small portion of the SAF, on the order of several kilometers.

3.3. Long-Term BSZ Seismicity

The BSZ is one of the most seismically active regions of southern California with frequent swarms and steady background activity. Since the early 1930s, the BSZ has accommodated five $M \geq 5.5$ events and 1179 $M \geq 3$

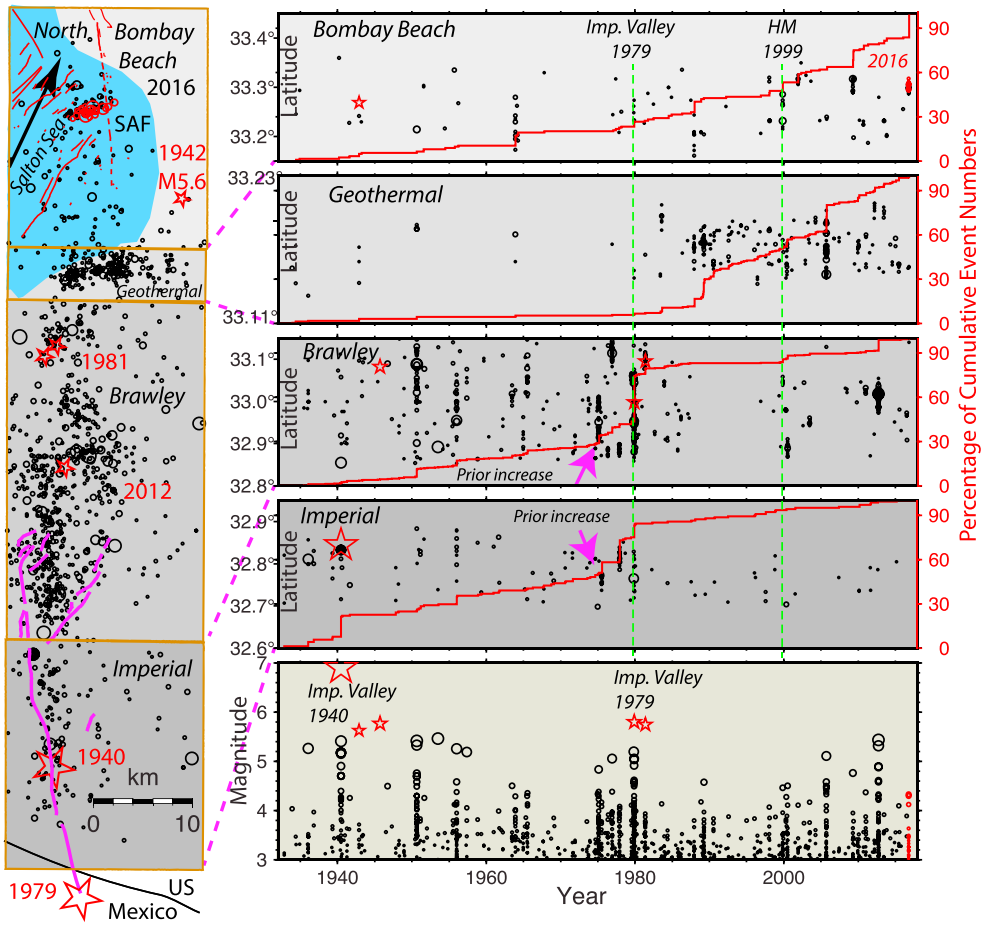

Figure 4. The 1930–2016 time-space evolution of $M \geq 3.0$ seismicity in the BSZ (black circles). The $M \geq 5.5$ earthquakes (red stars) and the 2016 cluster (red circles). (left) a map view (map rotated 26°NE) showing (1) Bombay Beach, (2) Geothermal; (3) Brawley; and (4) Imperial areas. (right) Temporal evolution of the seismicity from 1930 to present. Individual events and the percent of cumulative event numbers in each box are plotted. The 2016 cluster as (red circles). (bottom) magnitude versus time for all $M \geq 3.0$ events in the BSZ; Imp. Valley—Imperial Valley.

events that often occur in swarms [*Johnson and Hutton,* 1982; *Hauksson et al.,* 2012; *Hauksson et al.,* 2013; *Chen and Shearer,* 2011]. Some of these swarms that were triggered by the 1979 M_w 6.5 Imperial Valley earthquake occurred over a ~80 km distance north of the international border, demonstrating that both static and dynamic triggering could easily occur in this area. To analyze the long-term rates of $M \geq 3.0$ earthquakes in the BSZ, we have divided the region into four zones (Imperial, Brawley, Geothermal, and Bombay Beach) (Figure 4).

The southernmost Imperial zone coincides with the northernmost segment of the Imperial Fault with a steady rate of seismicity to the east of the fault. The only change in the seismicity rate in this zone occurred during the 5 years before the 1979 M_w 6.5 earthquake. In the central Brawley zone *Chen and Shearer* [2011] found numerous different clusters with more than 50 events each from 1981 to 2009. It also accommodated a seismicity increase before the 1979 event as well as the M_w 5.8 Westmoreland swarm in 1981 and the M_w 5.4 Brawley swarm in 2012 [*Hauksson et al.,* 2012].

The geothermal zone, near the south shore of the Salton Sea is characterized by swarms of seismicity that may be related to exploitation of the geothermal energy [*Llenos and Michael,* 2016]. The seismicity rate in this zone increased abruptly in the mid-1980s as geothermal energy production was initiated. In particular, the 2005 Obsidian Butte swarm produced more than 1500 recorded events, the largest being M_w 5.1, and extended for a distance of ~10 km. This swarm also coincided in time with a shallow slow slip event detected on global positioning systems (GPS) and interferometric synthetic aperture radar instruments [*Lohman and McGuire,* 2007].

In the Bombay Beach zone close to the southern terminus of the SAF, the rate of $M \geq 3.0$ earthquakes was ~0.7 events per year from 1930 to 1979 but has been ~2.5 events per year since then. Only one 1942 *M*5.6 earthquake and no *M*4 events were reported in this zone before the 1979 Imperial Valley earthquake. Because no felt reports are available for the 1942 *M*5.6 Calipatria event, it could be a mislocated aftershock of the 1942 M_w 6.6 Carrizo Mountain earthquake that occurred nine hours earlier, located about 50 km to the southwest [*Hileman et al.,* 1973]. The three clusters analyzed in this paper are part of an increase in the rate of $M \geq 3.0$ earthquakes that began in 1979. *Gomberg et al.* [2001] and *Hough and Kanamori* [2002] reported that triggered *M*4.4, *M*4.7, and several smaller earthquakes occurred about 10 km south of the three clusters, immediately following the 1999 M_w 7.1 Hector Mine earthquake. Similar increases in seismicity rates were not observed in the zones further to the south.

4. Discussion

4.1. Implications for Triggering of SAF

The risk and societal implications of a major earthquake rupturing the southern SAF would be enormous, with potentially thousands of casualties and damage in the hundreds of millions of dollars [*Jones et al*., 2008]. The rupture could extend for a distance of 300 km or more, from the Salton Sea to Palmdale or even Parkfield, and cause significant shaking in the Inland Empire and Los Angeles metropolitan areas. The relative likelihood of the occurrence of such an event is considered to be high because the southern SAF ruptured last in a major earthquake more than 320 years ago [*Rockwell et al.,* 2016]. Also, the average recurrence rate of large earthquakes on the southern SAF is ~180 years based on a slip rate of about 20 mm/yr in Coachella Valley from paleoseismological data [*Philibosian et al*., 2011].

When each of the three clusters occurred, there was heightened concern about their ability to trigger a major earthquake along the southernmost SAF. The California Office of Emergency Services and the USGS issued official warnings stating that there was a higher likelihood for a major SAF following these events lasting for a few days [*Goltz*, 2015]. The thought was that the rate of seismicity adjacent to the SAF suddenly had increased from almost zero to tens of events per day, and such clusters could be foreshocks [*Agnew and Jones,* 1991]. In addition, these events were perturbing the state of stress in and around the SAF.

The fact that swarm activity has so far triggered neither small nor large earthquakes on the SAF may reflect that the southern SAF is not ready for a major earthquake or that the imparted stress perturbations from the swarm events are either negative or not large enough. While the complex patterns of positive and negative Coulomb stress on the SAF reach high amplitudes in the immediate vicinity of the swarm events, they quickly decay with distance from the swarms. The imparted Coulomb stress changes reach comparable levels over a very limited part of the SAF as those caused by the M_w 7.3 1992 Landers sequence and M_w 7.1 1999 Hector Mine earthquake, which also did not trigger a rupture on the SAF [*Harris and Simpson,* 1992; *Stein et al.,* 1992; *Kilb,* 2003].

The strength of the southern SAF is not well understood but geodetic data provide some constraints. *Lindsey and Fialko* [2013] who used synthetic aperture radar and GPS measurements pointed out that limited sections of the Coachella SAF segment accommodated surface creep of 2 to 4 mm/yr extending to a depth of ~3 km. They also inferred that the SAF is seismogenic and locked, extending from ~3 km to ~14 km depth, where there is also no seismicity. Tectonic tremor that could be an indication of localized aseismic deformation has not been reported in this region.

Furthermore, the exact location and geometry of the offshore part of the SAF is not well mapped and may form up to a 1 km wide shear zone [*Janecke and Markowski*, 2013]. This lack of knowledge about the actual southern extent of the SAF is a critical factor for hazard considerations. If the SAF ends at Bombay Beach, the impact of the swarms 5 km south of that point will always be small. The longer-term change in seismicity rate may then be a more significant reason for concern, but there is no obvious way to calculate the corresponding change in hazard.

The geometry of the offshore aseismic hinge faults in the Salton Sea that exhibit mostly normal faulting does not match the orientations of the faults that rupture in the three clusters. The difference in strike is ~20°, with the step over faults striking more to the north than the nodal planes of the focal mechanisms. Thus, the *M*6 normal-faulting event postulated by *Brothers et al.* [2011] may not be the most likely event to affect the SAF.

The reverse scenario may be equally probable, where large ruptures on the SAF trigger ruptures on these hinge faults, but so far, there is not enough available data to discriminate between these different cases.

4.2. Driving Mechanisms

The three observed clusters exhibit spatial migration patterns indicative of aseismic creep events as a driver of the clusters. Previously, *Vidale and Shearer* [2006] argued that most southern California swarms are driven by aseismic slip events, although the supporting geodetic data are very limited. Similar features and a migration velocities between 1 to 2 km/h as well as crustal deformation were observed by *Lohman and McGuire* [2007] for the 2005 *Mw* 5.1 Obsidian Butte swarm (Figure 1). It occurred 15 km to the south, near the south shore of the Salton Sea. If slow creep was occurring during the three clusters, the aseismically imparted Coulomb stress changes on the SAF could be larger but would be applied more gradually than stresses from the earthquakes.

Although these small clusters did not themselves cause significant change to the stresses on the SAF, they may be relevant in that they reflect a longer-term change in seismicity rate of the northern BSZ. For most of its recorded history, the northernmost part of the BSZ has been very quiet. The rate of $M \geq 3.0$ earthquakes increased after the 1979 Imperial Valley and has increased again in the last 15 years including an increase in the largest magnitudes of the swarms (Figure 4). This change in rate is similar to that seen in the southern BSZ prior to the 1979 *M*6.5 earthquake on the Imperial Fault.

5. Conclusions

The 2001, 2009, and 2016 earthquake clusters that may have been caused by aseismic creep did not trigger a major rupture on the SAF because the imparted stress changes were too small or the SAF is not as close to failure as expected. The mapped fault structures in the Salton Sea are capable of accommodating large events. However, they are not seismically active and have different strike and slip orientation than the currently unmapped seismically active structures in the Salton Sea. The 1979 M_w 6.5 Imperial Valley and 1999 M_w 7.1 Hector Mine earthquakes appear to have caused enough stress change in the region to initiate an increase in the seismicity rate in the region, which demonstrates that the BZS is indeed susceptible to earthquake triggering. In contrast, the SAF appears to be firmly locked. Because seismic activity reflects ongoing deformation, and mechanisms of earthquake triggering are poorly understood, swarm activity near the SAF is generally a reason for concern. Real-time seismic monitoring and rapid identification of cluster parameters, such as migration velocities of swarms and Coulomb stress changes, may aid in making future near real-time hazards estimates.

Acknowledgments
Supported by USGS/NEHRP: G16AP00147, National Science Foundation (NSF): EAR-1550704, and Southern California Earthquake Center (contribution 7176) and funded by NSF EAR-1033462 and USGS G12AC20038. Figures done with PMG from *Wessel et al.* [2013]. Used data are from the Caltech/USGS SCSN; doi:10.7914/SN/CI; stored at Southern California Earthquake Data Center (SCEDC) doi:10.7909/C3WD3xH1.

References

Agnew, D. C., and L. M. Jones (1991), Prediction probabilities from foreshocks, *J. Geophys. Res.*, *96*, 11,959–11,971, doi:10.1029/91JB00191.

Bent, A., D. V. Helmberger, R. J. Stead, and P. Ho-Liu (1989), Waveform modeling of the November 1987 Superstition Hills Earthquakes, *Bull. Seismol. Soc. Am.*, *79*(2), 500–514.

Brothers, D. S., N. W. Driscoll, G. M. Kent, A. J. Harding, J. M. Babcock, and R. L. Baskin (2009), Tectonic evolution of the Salton Sea inferred from seismic reflection data, *Nat. Geosci.*, *2*, 581–584, doi:10.1038/ngeo590.

Brothers, D., D. Kilb, K. Luttrell, N. Driscoll, and G. Kent (2011), Loading of the San Andreas fault by flood-induced rupture of faults beneath the Salton Sea, *Nat. Geosci.*, *4*(7), 486–492, doi:10.1038/ngeo1184.

Chen, X., and P. M. Shearer (2011), Comprehensive analysis of earthquake source spectra and swarms in the Salton Trough, California, *J. Geophys. Res.*, *116*, B09309, doi:10.1029/2011JB008263.

Clinton, J. F., E. Hauksson, and K. Solanki (2006), An evaluation of the SCSN moment tensor solutions: Robustness of the M_W magnitude scale, style of faulting, and automation of the method, *Bull. Seismol. Soc. Am.*, *96*(5), 1689–1705, doi:10.1785/0120050241.

Felzer, K. R., and E. E. Brodsky (2006), Decay of aftershock density with distance indicates triggering by dynamic stress, *Nature*, *441*, 735–738, doi:10.1038/nature04799.

Fuis, G. S., D. S. Scheirer, V. E. Langenheim, and M. D. Kohler (2012), A new perspective on the geometry of the San Andreas Fault in southern California and its relationship to lithospheric structure, *Bull. Seismol. Soc. Am.*, *102*(1), 236–251, doi:10.1785/0120110041.

Goltz, J. D. (2015), A further note on operational earthquake forecasting: An emergency management perspective, *Seismol. Res. Lett.*, *86*(5), 1231–1233, doi:10.1785/0220150080.

Gomberg, J., P. Reasenberg, P. Bodin, and R. Harris (2001), Earthquake triggering by transient seismic waves following the Landers and Hector Mine, California earthquakes, *Nature*, *411*, 462–466, doi:10.1038/35078053.

Hanks, T. (1992), Small earthquakes, tectonic forces, *Science*, *256*, 1430–1432, doi:10.1126/science.256.5062.1430.

Hardebeck, J. L., and P. M. Shearer (2003), Using S/P amplitude ratios to constrain the focal mechanisms of small earthquakes, *Bull. Seismol. Soc. Am.*, *93*(6), 2434–2444.

Harris, R. A., and R. W. Simpson (1992), Changes in static stress on southern California faults after the 1992 Landers earthquake, *Nature*, *360*, 251–254, doi:10.1038/360251a0.

Harris, R., R. Simpson, and P. Reasenberg (1995), Influence of static stress changes on earthquake locations in southern California, *Nature*, *375*, 221–224, doi:10.1038/375221a0.
Hauksson, E. (2000), Crustal structure and seismicity distributions adjacent to the Pacific and north America plate boundary in southern California, *J. Geophys. Res.*, *105*, 13,875–13,903, doi:10.1029/2000JB900016.
Hauksson, E., W. Yang, and P. M. Shearer (2012), Waveform relocated earthquake catalog for Southern California 1981 to June 2011, *Bull. Seismol. Soc. Am.*, *102*(5), doi:10.1785/0120120010.
Hauksson, E., et al. (2013), Report on the August 2012 Brawley earthquake swarm in Imperial Valley, southern California, *Seismol. Res. Lett.*, *84*, 177–189, doi:10.1785/0220120169.
Helmstetter, A. (2003), Is earthquake triggering driven by small earthquakes?, *Phys. Rev. Lett.*, *91*(5), 058,501, doi:10.1103/PhysRevLett.91.058501.
Hileman, J. A., C. R. Allen, and J. M. Nordquist (1973), Seismicity of the southern California region, 1 January 1932 to 31 December 1972, Seismological Laboratory, 487 pp., California Institute of Technology, Pasadena, California.
Hill, D. P., et al. (1993), Seismicity remotely triggered by the magnitude 7.3 Landers, California, earthquake, *Science*, *260*, 1617–1623.
Hough, S. E., and H. Kanamori (2002), Source properties of Earthquakes near the Salton Sea triggered by the 16 October 1999 *M* 7.1 Hector Mine, California, Earthquake, *Bull. Seismol. Soc. Am.*, *92*(4), 1281–1289.
Hudnut, K. W., L. Seeber, and J. Pacheco (1989), Cross-fault triggering in the November 1987 superstition hills earthquake sequence, southern California, *Geophys. Res. Lett.*, *16*, 199–202, doi:10.1029/GL016i002p00199.
Janecke, S. U., and D. Markowski (2013), New structures from the southern tip of the San Andreas fault zone near Durmid Hill: 2013 SCEC Annual Meeting poster, pp. 199. [Available at http://www.scec.org/meetings/2013am/SCEC2013Proceedings.pdf.]
Jennings, C. W., and W. A. Bryant (2010), Fault activity map of California. *Geologic Data Map No. 6, California Geological Survey, Sacramento, Calif.*
Johnson, C. E., and D. P. Hill (1982), Aftershocks and pre-earthquake seismicity, *U.S, Geol. Surv. Prof. Pap.*, *1254*, 15–24.
Johnson, C. E., and L. K. Hutton (1982), Seismicity of the Imperial Valley, in The Imperial Valley, California, earthquake of October 15, 1979, *U.S, Geol. Surv. Prof. Pap.*, *1254*, 59–76.
Jones, L. M. (1984), Foreshocks (1966–1980) in the San Andreas System, California, *Bull. Seismol. Soc. Am.*, *74*, 1361–1380.
Jones, L. M., et al. (2008), The ShakeOut Scenario: U.S. Geological Survey Open-File Report 2008-1150 and California Geological Survey Preliminary Report 25. [Available at http://pubs.usgs.gov/of/2008/1150/.]
Kilb, D. (2003), A strong correlation between induced peak dynamic Coulomb stress change from the 1992 *M*7.3 Landers earthquake and the hypocenter of the 1999 *M*7.1 Hector Mine, California, earthquake, *J. Geophys. Res.*, *108*(B1), 2012, doi:10.1029/2001JB000678.
Kilb, D., J. S. Gomberg, and P. Bodin (2000), Triggering of earthquake aftershocks by dynamic stresses, *Nature*, *408*, 570–574.
Lindsey, E. O., and Y. Fialko (2013), Geodetic slip rates in the southern San Andreas Fault system: Effects of elastic heterogeneity and fault geometry, *J. Geophys. Res. Solid Earth*, *118*, 689–697, doi:10.1029/2012JB009358.
Llenos, A. L., and A. J. Michael (2016), Characterizing potentially induced earthquake rate changes in the Brawley seismic zone, Southern California, *Bull. Seismol. Soc. Am.*, *106*(5), 2045–2062, doi:10.1785/0120150053.
Lohman, R. B., and J. J. McGuire (2007), Earthquake swarms driven by aseismic creep in the Salton Trough, California, *J. Geophys. Res.*, *112*, B04405, doi:10.1029/2006JB004596.
Marsan, D. (2005), The role of small earthquakes in redistributing crustal elastic stress, *Geophys. J. Int.*, *163*(1), 141–151, doi:10.1111/j.1365-246X.2005.02700.x.
Meier, M.-A., M. Werner, J. Woessner, and S. Wiemer (2014), A search for evidence of secondary static stress triggering during the 1992 M_w7.3 Landers, California, earthquake sequence, *J. Geophys. Res. Solid Earth*, *119*, 3354–3370, doi:10.1002/2013JB010385.
Michael, A. J. (2012), Fundamental questions of earthquake statistics, source behavior, and the estimation of earthquake probabilities from possible foreshocks, *Bull. Seismol. Soc. Am.*, *102*, 2547–2562, doi:10.1785/0120090184.
Philibosian, B., T. E. Fumal, and R. Weldon (2011), San Andreas Fault earthquake chronology and Lake Cahuilla history at Coachella, California, *Bull. Seismol. Soc. Am.*, *101*(1), 13–38.
Rockwell, T., K. Scharer, and T. Dawson (2016), Earthquake geology and paleoseismology of major strands of the San Andreas fault system, in *Applied Geology in California*, *Association of Environmental and Engineering Geology Special Publication*, vol. 26, edited by R. Anderson and R. Ferriz.
Sahakian, V., A. Kell, A. Harding, N. Driscoll, and G. Kent (2016), Geophysical evidence for a San Andreas subparallel transtensional fault along the Northeastern Shore of the Salton Sea, *Bull. Seismol. Soc. Am.*, *106*(5), 1963–1978, doi:10.1785/0120150350.
Scholz, C., (2002), *The Mechanics of Earthquakes and Faulting*, Cambridge Univ. Press, Cambridge, U. K., doi:10.1017/CBO9780511818516.
Stein, R. S., G. C. P. King, and J. Lin (1992), Change in failure stress on the southern San Andreas fault system caused by the 1992 Magnitude = 7.4 Landers earthquake, *Science*, *258*, 1328–1332.
Thurber, C. H. (1993), Local earthquake tomography: Velocities and Vp/Vs—Theory, in *Seismic Tomography: Theory and Practice*, edited by H. M. Iyer and K. Hirahara, pp. 563–583 , Chapman and Hall, London.
Vidale, J. E., and P. M. Shearer (2006), A survey of 71 earthquake bursts across southern California: Exploring the role of pore fluid pressure fluctuations and aseismic slip as drivers, *J. Geophys. Res.*, *111*, B05312, doi:10.1029/2005JB004034.
Waldhauser, F., and W. L. Ellsworth (2000), A double-difference earthquake location algorithm: Method and application to the northern Hayward fault, California, *Bull. Seismol. Soc. Am.*, *90*(6), 1353–1368.
Wang, R., F. Lorenzo-Martín, and F. Roth (2006), PSGRN/PSCMP—A new code for calculating co-and post-seismic deformation, geoid and gravity changes based on the viscoelastic-gravitational dislocation theory, *C. R. Geosci.*, *32*(4), 527–541.
Wessel, P., W. H. F. Smith, R. Scharroo, J. F. Luis, and F. Wobbe (2013), Generic Mapping Tools: Improved version released, *Eos Trans. AGU*, *94*, 409–410, doi:10.1002/2013EO450001.
Yang, W., and E. Hauksson (2013), The tectonic crustal stress field and style of faulting along the Pacific North America Plate boundary in Southern California, *Geophys. J. Int.*, *194*(1), 100–117, doi:10.1093/gji/ggt113.
Yang, W., E. Hauksson, and P. Shearer (2012), Computing a large refined catalog of focal mechanisms for southern California (1981–2010): Temporal stability of the style of faulting, *Bull. Seismol. Soc. Am.*, *102*(3), 1179–1194, doi:10.1785/0120110311.